Thermochimica Acta 473 (2008) 61–67

Contents lists available at ScienceDirect

Thermochimica Acta

journal homepage: www.elsevier.com/locate/tca

A study on the kinetics of hydrogen reduction of molybdenum disulphide powders

M. Mehdi Afsahi [a,b,*], Morteza Sohrabi [a], R. Vasant Kumar [b], Habib Ale Ebrahim [a]

[a] Amirkabir University of Technology, Department of Chemical Engineering, Tehran 15914, Iran
[b] University of Cambridge, Department of Materials Sciences and Metallurgy, Cambridge CB2 3QZ, UK

ARTICLE INFO

Article history:
Received 20 November 2007
Received in revised form 5 April 2008
Accepted 8 April 2008
Available online 23 April 2008

Keywords:
Molybdenum disulphide
Hydrogen
Kinetics
Reduction
Gas–solid reaction

ABSTRACT

In order to achieve direct reduction of molybdenite in presence of a sulphur scavenger such as CaO such that SO_2 emission is completely avoided, it is important to maximise the rate of the partial reaction involving molybdenite and hydrogen (without lime) given the low thermodynamic driving force for this reaction. Accordingly, reaction of molybdenum disulphide powders with hydrogen was investigated by thermogravimetric method. Effect of temperature and concentration on the reaction rate was studied under such conditions that resistance to mass transfer arising from external film, between particles and intra-grain was negligible. The operating temperature ranged between 973 and 1173 K while the hydrogen concentration was varied between 30 and 100%. The experimental data obtained under the above conditions were analyzed by applying "the shrinking unreacted core model". The reduction reaction was found to be first order with respect to the gaseous reactant. Pre-exponential factor and activation energy have been determined to be 3.91×10^3 cm min^{-1} and 139.0 kJ mol^{-1}, respectively. Activation energy obtained from a fitted model, agreed well with the values determined from the model-free methods using isothermal measurements.

1. Introduction

Commercial source of molybdenum metal and molybdenum compounds is MoS_2. Molybdenum disulphide, in addition to its natural occurrence, can be prepared synthetically by several routes including direct union of elements in pure nitrogen [1], thermal decomposition of ammonium tetrathiomolybdate or molybdenum trisulphide [2–7], and by reaction between MoO_3 and H_2S or H_2S/H_2 mixtures [8]. Such preparative techniques result in hexagonal crystalline MoS_2, by far the most common form, the rhombohedral form is found in nature, and may be synthesized [6]. Natural and synthetic MoS_2 of both crystalline types possess lubricant properties, but the natural hexagonal material is preferred when cost and overall performance are considered. The excellent lubricant properties of MoS_2 are attributed to the large spacing and weak van der Waals bonding between S–Mo–S sandwich layers. Frictional behaviour and other factors influencing the performance of MoS_2 as a lubricant have been discussed in review papers [9–11] and a number of research papers [12–17].

Conventional method for producing molybdenum metal is based upon roasting of molybdenite concentrate, followed by purification of the resultant oxide (MoO_3), and a final step of reduction of purified molybdenum oxide with hydrogen [18]. Overall process suffers from disadvantages such as, high number of processing steps, environmental pollution by SO_2 emission from roasting of MoS_2, and low yield due to loss of materials during purification. Industrial importance of molybdenum metal on one hand and processing difficulties on the other have motivated the scientist to search for more efficient methods for producing molybdenum metal.

One such method is based on directly reducing molybdenite in presence of a sulphur scavenger agent such as CaO [19–24], and the reaction can be described as

$$MoS_2(s) + 2H_2(g) + 2CaO(s) \rightarrow Mo(s) + 2CaS(s) + 2H_2O(g) \quad (1)$$

It is possible to consider that reaction (1) is made up the following two partial reactions (2) and (3):

$$MoS_2(s) + 2H_2(g) \rightarrow Mo(s) + 2H_2S(g) \quad (2)$$

$$H_2S(g) + CaO(s) \rightarrow CaS(s) + H_2O(g) \quad (3)$$

The standard-free energy changes and the corresponding equilibrium constants for the above three reactions are given in Table 1, in the temperature range of 973–1273 K [25]. Reaction (2) is

* Corresponding author at: University of Cambridge, Department of Materials Sciences and Metallurgy, Cambridge CB2 3QZ, UK. Tel.: +44 7790066854; fax: +44 1223 334567.
E-mail addresses: mma50@cam.ac.uk, mmafsahi@gmail.com (M. Mehdi Afsahi).

0040-6031/$ – see front matter © 2008 Elsevier B.V. All rights reserved.
doi:10.1016/j.tca.2008.04.009

Table 1
The standard-free energy changes and the equilibrium constants for reactions (1)–(3)

T (K)	ΔG° (kJ mol^{-1})			K (equilibrium constant)		
	Reaction (1)	Reaction (2)	Reaction (3)	Reaction (1)	Reaction (2)	Reaction (3)
973	13.8	136.1	−61.1	0.2	4.9E−8	3.7E6
1073	5.4	127.9	−61.2	0.5	5.9E−7	9.1E5
1173	−2.8	119.8	−61.2	1.3	4.6E−6	2.9E5
1273	−10.8	112.0	−61.4	2.8	2.5E−5	1.1E5

clearly the least favoured reaction thermodynamically, the driving force can only be maintained by keeping the P_{H_2S}/P_{H_2} at very low values, e.g. the equilibrium value of ratio is 2.5×10^{-5} at 1273 K. The main driving force for the desired reaction (1) is thus derived from reaction (3) due to the excellent scavenging properties of CaO. For the overall reaction, it can be noted that the driving force increases marginally with increasing temperature. The equilibrium value of P_{H_2S}/P_{H_2} at 1273 K, for the reaction (1) is 2.8, suggesting that MoS_2 can be reduced to Mo in presence of CaO, more readily than without it. Fixing S with CaO, also has the potential to eliminate the formation of H_2S, which is toxic and polluting replacing it with benign H_2O as the gaseous product.

This low driving force for direct reduction with hydrogen is not specific to MoS_2 but other sulphide compounds also suffer from the same problem. Presence of a sulphur adsorbent with large equilibrium constant eliminates the H_2S gas from the reactions media and shifts the reaction to the right.

It is envisaged that in future, especially when H_2 is available through use of non-C energy, there will be incentive for most or many metallurgical reductions to be carried out with H_2 rather than with C-based fuels.

Given the future interest in hydrogen economy and in the anticipated massive reduction in C emissions, it is surprising that apart from a few investigations [26–28], no significant work has been performed during the recent years in this topic.

To model the reaction (1) intrinsic kinetic parameters of reactions (2) and (3) can be helpful in designing suitable process and equipment. The aim of the present study is to obtain the intrinsic kinetic parameters of reaction (2) towards elucidating detailed fundamental mechanisms.

There is no published paper in the literature on the kinetic parameters for the hydrogen reduction of MoS_2 except for modelling research work by the present authors that has been recently submitted (Mehdi Afsahi et al., A model for the intrinsic kinetic of the direct reduction of MoS_2 with hydrogen). For other metals such as Co, Ni and Cu, a few investigations have been reported for reducing sulphide with hydrogen [29–32].

2. Experimental

2.1. Materials

MoS_2 powder was supplied by Alpha Aesar Company (melting point 1185 °C, hexagonal structure, 99% purity and −325 mesh size), helium gas with purity of 99.999% was used as protective gas during the heating of the sample before starting the reaction and during cooling of the furnace at the end of the reaction. Hydrogen used was of extra pure gas grade (with less than 10 ppm impurity). Since MoS_2 reacts easily with oxygen at the elevated temperatures, and the amounts of MoS_2 in the majority of experiments were quite low (*ca.* 5 mg) the complete elimination of oxygen and water vapour from the gas stream was crucial. Two traps were, therefore, used in the gas line prior to the furnace.

2.2. Apparatus and procedure

Experiments were performed, using a thermogravimetric apparatus (Shimadzu TGA-50, Japan) with the accuracy of 1 μg. A schematic diagram of the experimental setup is shown in Fig. 1. A ceramic tube with inner diameter of 18 mm placed in an electric furnace was applied as a reactor. The MoS_2 powders were placed in a quartz cell 13 mm inner diameter and 4 mm height. In order to make a shallow powder bed, the majority of experiments were carried out with 5 mg of powders. The cell containing the sample was suspended from an arm of the balance by a platinum wire. The temperature of the furnace was measured by a thermocouple (S-type) placed under the cell. In order to control the gas flow rate further, in addition to the rotary flow meters situated before the furnace, a soap bubble flow meter was also placed after the furnace.

Prior to the experimental runs, the balance was calibrated using standard weights and the thermocouple was checked by dropping a tiny piece of platinum metal hanging from a silver wire (mp: 962 °C). The quartz cell containing the weighed sample was suspended from the balance. The furnace was then brought to the proper position and the sample was heated under a continuous flow of 70 ml min^{-1} of helium gas with a temperature increasing at a rate of 30 K min^{-1} until the set point was reached. Five minutes later helium gas flow was switched to that of hydrogen and the reduction in weight of the sample was recorded every 2 s. At the end of each run, the hydrogen flow was turned off and the sample was allowed to cool down under helium atmosphere. In all experiments the gas was entered from the top of the furnace and was allowed to leave via the bottom of the apparatus.

3. Results and discussion

3.1. Introduction

It is known [33] that molybdenum disulphide will not be solubilised by moisture, in fact it dissolves only in strongly oxidizing acids (e.g. aqua regia) to give molybdenum(VI) compounds. In inert atmosphere as in He, MoS_2 is stable and can decompose to Mo_2S_3 and metallic molybdenum only under vacuo at elevated temperature >1473 K. Heating in air at 773 K produces MoO_3. Reduction with hydrogen at 1373 K has been reported to yield Mo_2S_3 [33].

3.2. Characterizations of the molybdenum sulphide

Particle size of as received molybdenum sulphide was −325 mesh. In order to reduce intra-grain diffusion resistance, the powder was ground for 1 h in a ball mill. To ensure that during grinding operation, oxidation of MoS_2 has not occurred, the powdered samples were examined by XRD. No changes in the characteristic peaks before and after grinding were observed. Particle size distribution of the ground powders was measured by a laser particle size analyzer (Cilas, Model 1064 Dry). Ground molybdenum sulphide had a narrow particle size distribution with an average size of 1.77 μm.

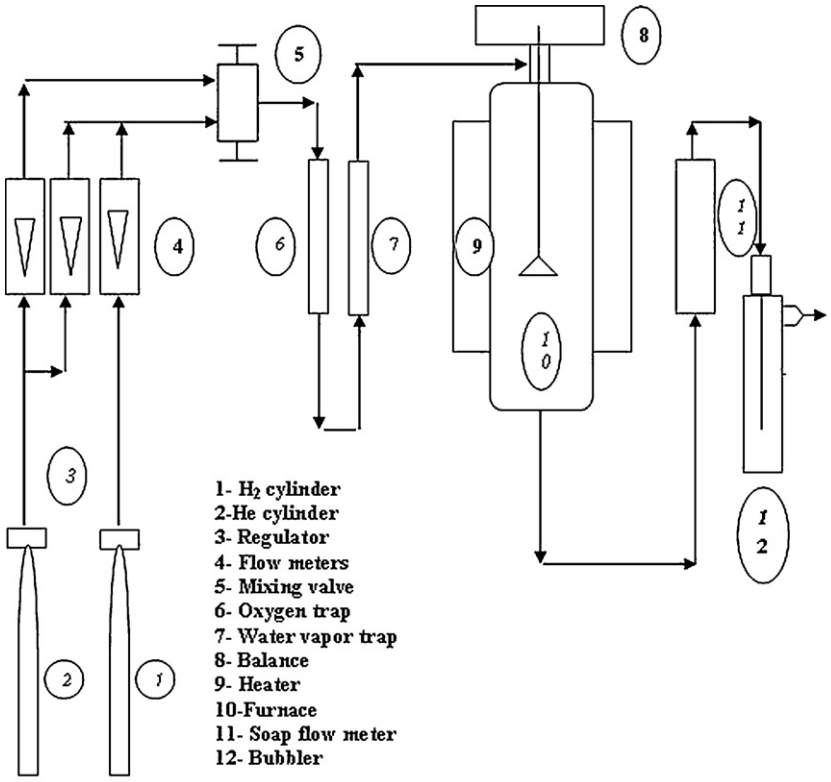

Fig. 1. Schematic diagram of the experimental system.

The scanning electron micrograph (JEOL 6340F FEG) was used to provide useful information concerning topography and morphology of the particles. Fig. 2 reveals that MoS_2 particles had irregular shapes and highly impervious structure. Fig. 3 indicates that the molybdenum disulphide consisted of flat shape particles.

The specific surface area of the ground powders was measured by BET method (TriStar 3000 V6.04 A) and was found to be $5.09\,m^2\,g^{-1}$. Thus MoS_2 powders are solid particles with each particle possessing a nonporous structure, hence, as reported there is a one-to-one relation between surface area and particle size [10].

3.3. Kinetic measurements

Intrinsic kinetic parameters should be determined under conditions where no mass transfer effects intrude the rate of the reaction. The effect of hydrogen flow rate on conversion at 1123 K is shown in Fig. 4 for a constant amount of sample (30 ± 1 mg). Progress of the reaction has been monitored by considering conversion (X). The conversion at any time $X(t)$ is defined as the weight loss of the sample divided by the theoretical maximum weight loss, i.e., when all the sulphur atoms are assumed to be removed from the sample. The error in the fraction converted at a given time is estimated as 0.03, arising from errors in

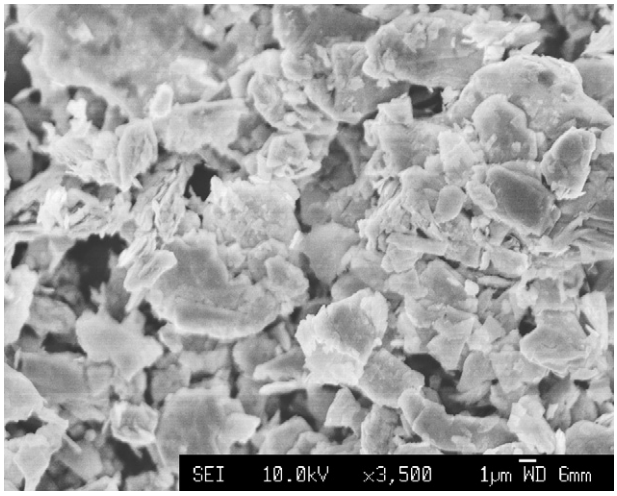

Fig. 2. Scanning electron micrograph showing the irregular and impervious surface of the MoS_2 particles before reaction.

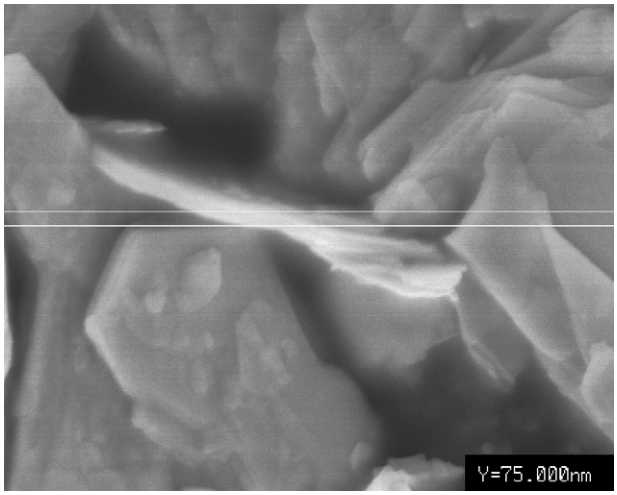

Fig. 3. Scanning electron micrograph showing that MoS_2 consists of flat plate particles with a width of 75 nm.

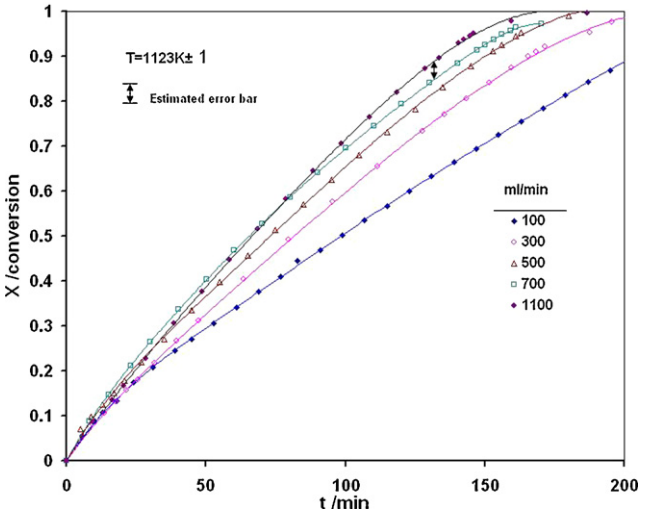

Fig. 4. Effect of hydrogen flow rate on conversion ($P_{H_2} = 0.82$ bar).

temperature, flow rate and weight measurements. Thus there is clear trend of increasing conversion with time as the hydrogen flow rate is increased from 100–300–500–700 ml min^{-1}, especially after 50 min of reduction time. At flow rates higher than 700 ml min^{-1}, the conversion is unaffected by increasing the flow rate within the experimental error. External mass transfer resistance can be reduced by increasing the rate of the gas flow. Critical flow rate, beyond which, no further effect on the reaction rate could be observed was determined to be 700 ml min^{-1}. This is considered sufficient to eliminate the external mass transfer resistance. All subsequent runs were, therefore, carried out at a slightly higher flow rate of 800 ml min^{-1}.

Intra-particle diffusion effects were reduced by evenly spreading the fine particles in the quartz cell. The effect of powder quantity on the reaction rate is shown in Fig. 5. There is an insignificant difference between the curves for the 5 mg and the 8 mg samples. Subsequent runs were, therefore, carried out using 5 mg of powders.

In order to demonstrate the reliable performance of the equipment, the data obtained from the thermogravimetric analysis have been presented directly without any smoothness in Fig. 5.

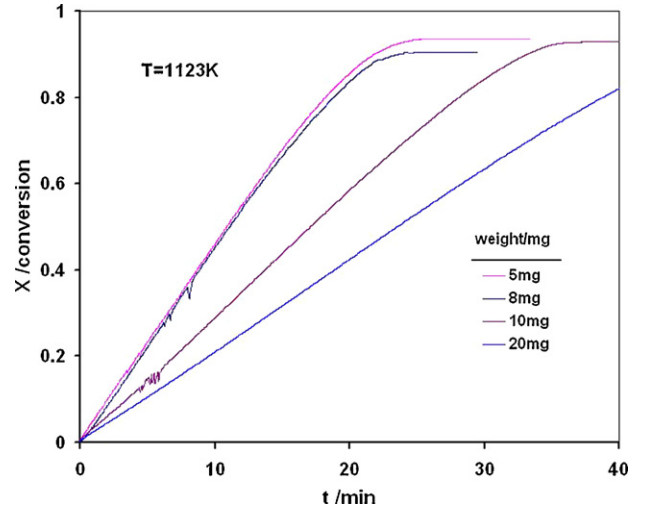

Fig. 5. Effect of sample weight on the conversion of molybdenum disulphide with hydrogen.

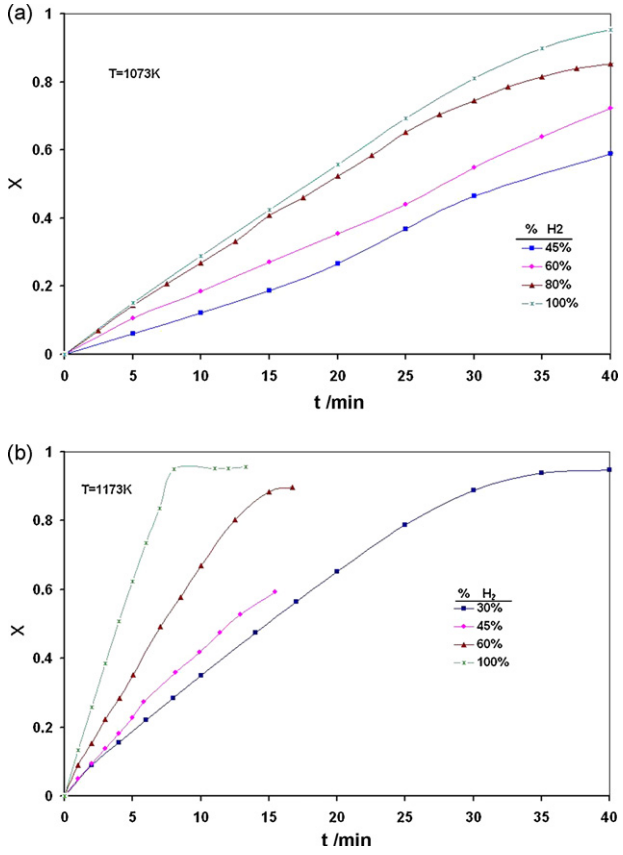

Fig. 6. Effect of hydrogen concentration on the rate of reaction (hydrogen flow rate: 800 cm^3/min; weight of sample: 5 mg; temperature: 1073 and 1173 K).

The effect of hydrogen concentration on the reaction rate within the range of 30–100% was investigated at two different temperatures, 1073 and 1173 K. The data are shown in Fig. 6a and b. The concentration of hydrogen was regulated by varying the flow rates of both hydrogen and helium while maintaining the total flow rate of gases at 800 ml min^{-1}.

The reaction temperature was varied within the range of 973–1173 K. The effect of temperature on the reaction of MoS_2 powders with pure hydrogen gas at 0.82 bar is shown in Fig. 7.

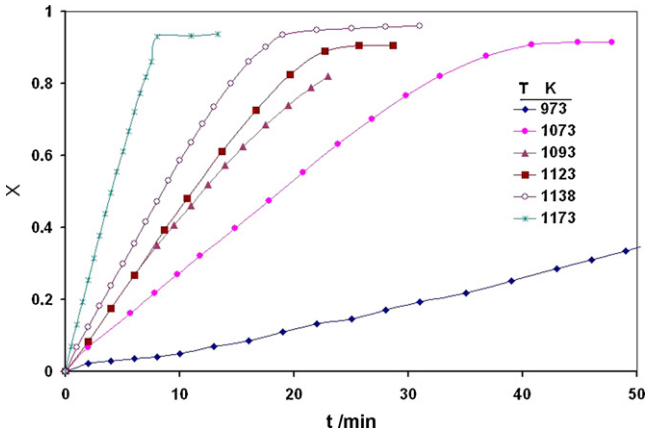

Fig. 7. Effect of temperature on the rate of reaction (5 mg sample of 1.77 μm average size of particles ($P_{H_2} = 0.82$ bar).

4. Interpretation of rate data

Some researchers [20,29–32] have reported the growth of filamentary products (or whiskers) in the reduction of metal sulphides such as nickel, cobalt and copper. However, in the present work, as is shown in Fig. 8, the product after reduction of MoS_2 powders is a porous material without any filament or whisker.

Since the starting particles are nonporous, experimental data may be analyzed by using the "shrinking unreacted core model" [34]. The relations describing such a model could be given as follows:

$$\mathrm{A(g)} + b\mathrm{C(s)} \rightarrow c\mathrm{C(g)} + d\mathrm{D(s)}$$

$$\left(\frac{bk}{\rho}\right)\left(C_{\mathrm{A}^0}^{n} - \frac{C_{\mathrm{C}^0}^{m}}{K_{\mathrm{e}}}\right)\left(\frac{A_{\mathrm{p}}}{F_{\mathrm{p}}V_{\mathrm{p}}}\right)t = 1-(1-X)^{1/F_{\mathrm{p}}} = g(X) \quad (4)$$

In the above equation, C_{A^0} and C_{C^0} are the bulk concentrations; n and m are the orders of reaction with respect to gaseous A and C, respectively. In this equation, b is the number of moles of solid reacted by 1 mol of gaseous reactant ($b = 1/2$ for reaction (1)); k and K_{e} are the reaction and equilibrium constants, respectively; ρ is the true density of MoS_2 particles; $g(X)$ is integrated form of the reaction model; A_{p} and V_{p} represent surface and volume of particles, respectively; F_{p} is the shape factor of particles and equal to 1, 2 and 3 for flat, cylindrical and spherical grains, respectively; t is the time and the term $(F_{\mathrm{p}}V_{\mathrm{p}}/A_{\mathrm{p}})$ is the characteristic dimension of the particles. This is equal to half of the thickness for a flat plate and radius for cylindrical and spherical particles ($(0.075/2)\times 10^{-6}$ m in this work).

The relation between conversion X and time may be, therefore, shown by the following equation:

$$X(t) = \frac{W_0 - W(t)}{W_0(M_{\mathrm{S}_2}/M_{\mathrm{MoS}_2})} = 2.4962(1 - W(t))/W_0 \quad (5)$$

In the above equation W_0 and $W(t)$ are the initial weight of the sample and the weight at time t (as measured by the thermogravimetric method). M_{MoS_2} and M_{S_2} are molecular weights of MoS_2 and the liberated sulphur, respectively.

When mass transfer resistances are eliminated, the concentration of gaseous product (C_{c}) on the solid surface may be assumed to be negligible and Eq. (4) could be simplified to

$$\left(\frac{bk}{\rho}\right)C_{\mathrm{A}^0}^{n}\left(\frac{A_{\mathrm{p}}}{F_{\mathrm{p}}V_{\mathrm{p}}}\right)t = 1-(1-X)^{1/F_{\mathrm{p}}} = g(X) \quad (6)$$

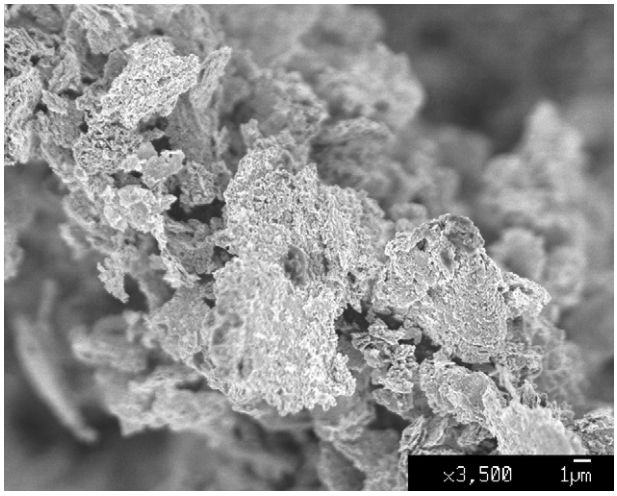

Fig. 8. Scanning electron micrograph showing the porous structure of the reaction product at 1123 K.

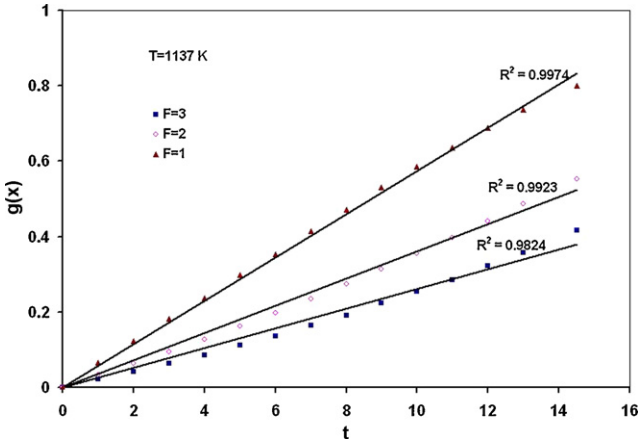

Fig. 9. Typical results of the reduction of MoS_2 for different values of shape factor.

Eq. (4) has been obtained based on the following assumptions:

(a) particles are nonporous;
(b) particles maintain their initial shape and size;
(c) the reaction is isothermal;
(d) impact of structural change of the particles on the progress of reaction is negligible.

By comparing the SEM images for product and reactant (Figs. 2, 3 and 8), it may be concluded that assumptions (a) and (b) is justified. This reaction is highly endothermic (+213 kJ mol^{-1} [25]), but since size of the particles are very small and also since small amount of particles is used in the experiments therefore isothermal reaction is an acceptable assumption.

Since as sulphur is removed from MoS_2 powders during the reaction, structural properties of particles such as density and porosity will also change, and this could affect the results.

The shape factor of a particle, provided that the mass transfer resistances are eliminated, can be determined from the slope of a straight line obtained by plotting the experimental values of $g(X)$ against the reaction time t. In Fig. 9, such plots, drawn at 1137 K have been given.

As it may be observed from this figure, the best correlation is obtained with $F_{\mathrm{p}} = 1$, corresponding to the particles having a flat shape. Similar conclusions can be made from the results at other temperatures and subsequently, confirmed by SEM images (Fig. 3). The effect of hydrogen concentration on the reaction rate at two different temperatures (1073 and 1173 K) was investigated. By plotting $g(X)$ versus time, according to Eq. (6), with $F_{\mathrm{p}} = 1$, a straight line is obtained (Fig. 10a and b) with a slope corresponding to

$$S = \left(\frac{bk}{\rho}\right)C_{\mathrm{A}^0}^{n}\left(\frac{A_{\mathrm{p}}}{F_{\mathrm{p}}V_{\mathrm{p}}}\right) \quad (7)$$

A plot of $\ln(S)$ versus $\ln(C_{\mathrm{A}^0})$ yields a straight line, the slope of which, determines the order of reaction (n). Values of n at 1073 and 1173 K are both close to unity. This may indicate that the reaction rate is first order with respect to hydrogen concentration (Fig. 11).

According to Eq. (6), at any selected temperature, a plot of $g(X)$ against t should yield a straight line with slope S from which the rate constant (k) at that particular temperature may be determined. Such curves are drawn in Fig. 12. Applying Arrhenius relation, from a plot of $\ln(k)$ versus T^{-1} (Fig. 13), the pre-exponential term and activation energy of the reaction were determined as 3.9×10^3 cm min^{-1} and 139.0 kJ mol^{-1}, respectively.

To verify the kinetic triplet derived in the present work (reaction model, pre-exponential factor and activation energy) a comparison

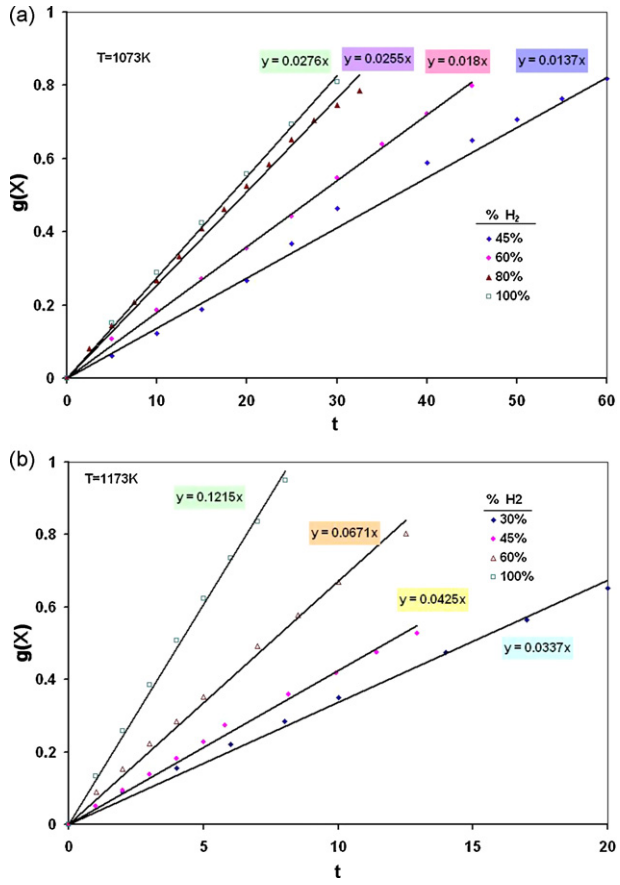

Fig. 10. Plot of integral conversion function against time at different concentrations of hydrogen (data from Fig. 6a and b).

has been made between the latter and those determined from the model-free method. A model-free equation for isothermal condition [35–37] may be considered as follows:

$$-\ln t_{X,i} = \ln\left(\frac{k_{0j}}{g_j(X)}\right) - \frac{E_X}{RT} \quad (8)$$

In the above equation, subscripts i and j refer to isothermal condition and the type of the model, respectively. $t_{X,i}$ is the time required to reach a certain conversion isothermally, k_0 and $g_j(X)$ represent pre-exponential factor and integrated form of the reaction model. Appling Eq. (8) to isothermal kinetic data within the range of $0.1 < X < 0.9$, values for E were obtained as a function of conversion with an average of 134.1 kJ mol^{-1} (Fig. 14).

This value is close to that determined previously, using shrinking unreacted core model.

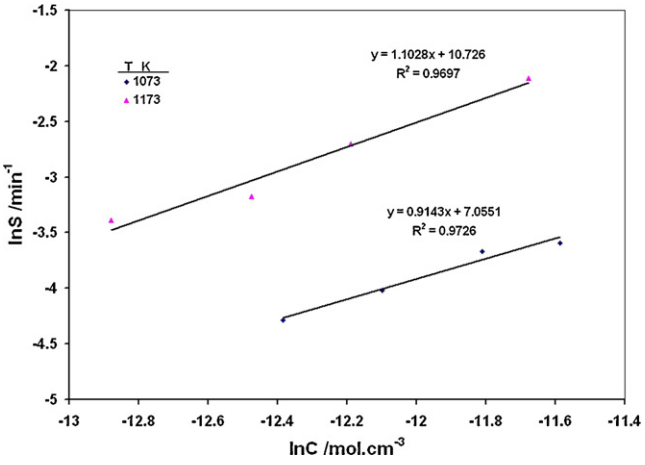

Fig. 11. Plot of ln(S) against ln(C) at two different temperatures (used for determining the order of the reaction).

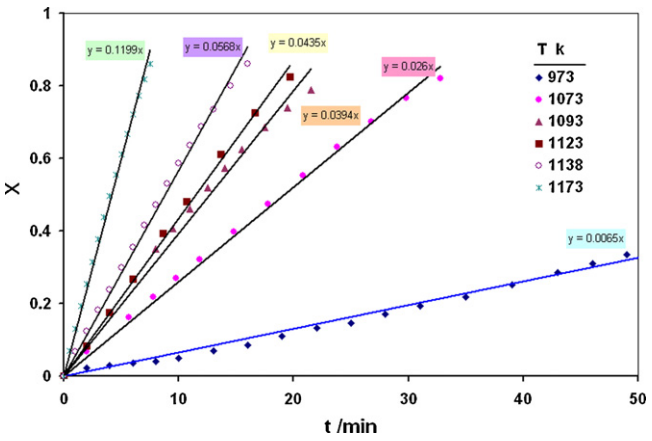

Fig. 12. Plot of conversion against time at different temperature (data from Fig. 7).

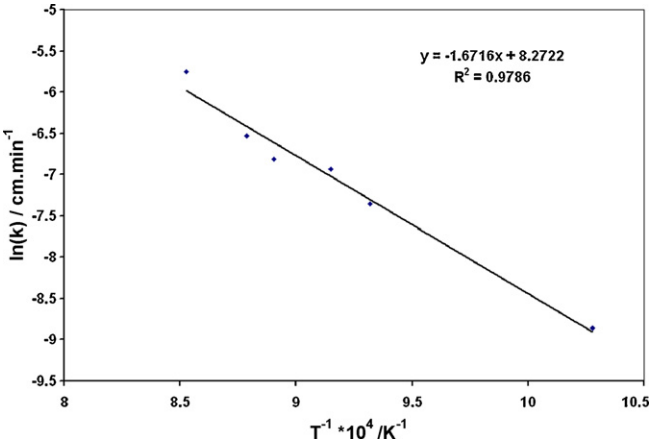

Fig. 13. Arrhenius plot for the reaction between MoS_2 powders and hydrogen (data from Fig. 12).

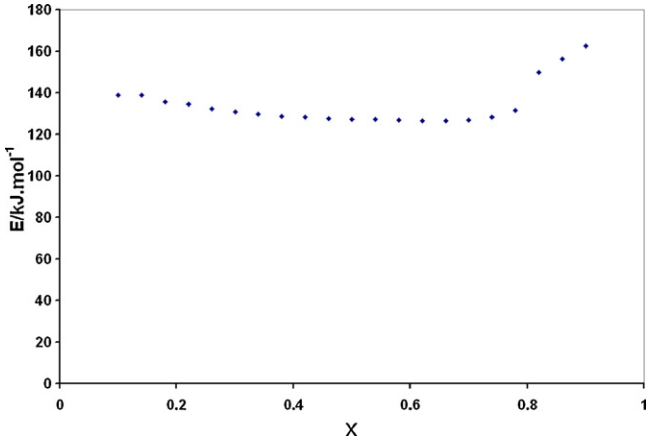

Fig. 14. Variation of the activation energy with conversion derived from model-free method applying isothermal kinetic data.

Similarity between the activation energy obtained from two different methods supports the kinetic triplet obtained from the shrinking unreacted core model.

It may be observed from Fig. 14 that dependency of activation energy on conversion is rather weak, decreasing at the early stages but increasing towards the end of the reaction. The changes in E with conversion may be described as follows.

Nucleation, nuclei growth and diffusion of the gaseous product provide the effective parameters that will determine the activation energy. Interaction of these phenomena is such that at the start of reaction, the activation energy is decreased. However, during a wide range of conversion, the latter remains almost unchanged. Finally, at the later stages of the reduction the activation energy is increased rapidly with conversion. This observation may be explained by noting that at the beginning of the reaction, the product layer imposes a negligible resistance to the overall rate. However, as the result of nuclei growth during the reaction, activation energy is decreased. On the other hand, at the final stages of the reaction, formation of a thick layer hinders the movement of gases towards the reaction zone, leading to higher activation energy.

In a previous study (Mehdi Afsahi et al., submitted for publication, A model for the intrinsic kinetic of the direct reduction of MoS_2 with hydrogen), the intrinsic kinetic parameters for reduction of flat pellets were determined, applying nucleation and growth models. The activation energy was found to be 135.4 kJ mol^{-1} which is close to the value determined in the present work.

5. Conclusions

In the present work variables affecting the reaction between MoS_2 powders and hydrogen gas were investigated. The data were analyzed using shrinking unreacted core model and compared with the free model method. The reaction rate constant was correlated by the following equation:

$$k = 3.91 \times 10^3 \exp\left(\frac{-1.67\times10^4}{T}\right) (\mathrm{cm\,min^{-1}})$$

It was found that the reaction rate was first order with respect to hydrogen gas concentration. This work is used as a foundation for further studies in the formation of Mo from molybdenite with hydrogen as the reducing agent and CaO as the sulphur scavenging agents.

References

[1] L. Chang, H. Yang, J. Li, W. Fu, Y. Du, K. Du, Q. Yu, J. Xu, M. Li, Nanotechnology 17 (2006) 3827–3831.
[2] S.K. Srivastava, B.N. Avasthi, J. Mater. Sci. 28 (18) (1993) 5032–5035.
[3] J. Chen, S.L. Li, Z.L. Tao, J. Alloys Compd. 356–357 (2003) 413–417.
[4] H.W. Wang, P. Skeldon, G.E. Thompson, G.C. Wood, J. Mater. Sci. 32 (2) (1997) 497–502.
[5] K. Du, W. Fu, R. Wei, H. Yang, S. Liu, S. Yu, G. Zou, Mater. Lett. 61 (27) (2007) 4887–4889.
[6] J.C. Wildervanck, F. Jellinek, Z. Anorg, Allgem. Chem. 328 (1964) 309–318.
[7] H.W. Wang, P. Skeldon, G.E. Thompson, G.C. Wood, J. Mater. Sci. Lett. 15 (6) (1996) 494–496.
[8] Y. Feldman, E. Wasserman, D.J. Srolovitz, R. Tenne, Science 267 (5195) (1995) 222–225.
[9] H.F. Barry, Lubricat. Eng. 33 (9) (1977) 475–480.
[10] J.P.G. Farr, Wear 35 (1975) 1–22.
[11] W.O. Winer, Wear 10 (1967) 422–452.
[12] J.M. Martin, in: D. Dowson (Ed.), Molybdenum Disulphide Lubrication, Tribology Series, vol. 35, 1999.
[13] W. Hai-Dou, X. Bin-Shi, L. Jia-Jun, Z. Da-Ming, Sci. Technol. Adv. Mater. 6 (5) (2005) 535–539.
[14] S. Watanabe, J. Noshiro, S. Miyake, Surf. Coat. Technol. 183 (2–3) (2004) 347–351.
[15] J. Xu, M.H. Zhu, Z.R. Zhou, Ph. Kapsa, L. Vincent, Wear 255 (1–6) (2003) 253–258.
[16] N.M. Renevier, J. Hamphire, V.C. Fox, J. Witts, T. Allen, D.G. Teer, Surf. Coat. Technol. 142–144 (2001) 67–77.
[17] L. Cizaire, B. Vacher, T. Le Mogne, J.M. Martin, L. Rapoport, A. Margolin, R. Tenne, Surf. Coat. Technol. 160 (2–3) (2002) 282–287.
[18] K. Othmer, Encyclopedia of Chemical Technology, fourth ed., John Wiley & Sons, New York, 1998.
[19] H. Kay, in: W.A. Krivsky (Ed.), High-Temperature Refractory Metals, Gordon and Breach, New York, NY, 1968, p. 33.
[20] F. Habashi, R. Dugdale, Metall. Trans. B 4 (1973) 1865–1871.
[21] P.M. Prasad, T.R. Mankhand, P. Suryaprakash Rao, Miner. Eng. 6 (8–10) (1993) 857–871.
[22] P. Suryaprakash Rao, P.M. Prasad, Mater. Trans. JIM 34 (12) (1993) 1229–1233.
[23] J.D. Ford, M.A. Fahim, Metall. Trans. B 6 (1975) 461–464.
[24] F. Habashi, B.J. Yostos, J. Metals 29 (7) (1977) 11–16.
[25] A. Roine, HSC Chemistry 6.0, Chemical Reaction and Equilibrium Software with Extensive Thermochemical Database and Flowsheet Simulation, Outokumpu Research Oy Information Center, August 2006.
[26] P.K. Tripathy, R.H. Rakhasia, Miner. Process. Extract. Metall. 115 (1) (2006) 8–14.
[27] P.M. Prasad, P. Surya Prakash Rao, S.N. Singh, A.J.K. Prasad, T.R. Mankhand, Metall. Mater. Trans. B: Process Metall. Mater. Process. Sci. 33 (3) (2002) 345–354.
[28] R. Padilla, M.C. Ruiz, H.Y. Sohn, Metall. Mater. Trans. B: Process Metall. Mater. Process. Sci. 28 (2) (1997) 265–274.
[29] R.E. Cech, T.D. Tiemann, TMS AIME 245 (1969) 1727–1733.
[30] M.A. Fahim, J.D. Ford, Can. J. Chem. Eng. 54 (1976) 578–583.
[31] T. Chida, J.D. Ford, Can. J. Chem. Eng. 55 (1977) 313–316.
[32] H.Y. Sohn, S. Won, Metall. Trans. B 16 (1985) 831–839.
[33] F. Ullmann, Ulmann's Encyclopedia of Industrial Chemistry, vol. 22, Wiley-VCH, Weinheim, 2003, p. 26.
[34] J. Szekely, J.W. Evans, H.Y. Sohn, Gas–Solid Reactions, Academic Press Inc., New York, 1976.
[35] S. Vyazovkin, C.A. Wight, Thermochim. Acta 340 (341) (1999) 53–68.
[36] S. Vyazovkin, Thermochim. Acta 355 (2000) 155–163.
[37] S. Vyazovkin, C.A. Wight, Chem. Mater. 11 (1999) 3386–3393.